Available online at www.sciencedirect.com

ScienceDirect

Materials Today: Proceedings 12 (2019) 329–334

materialstoday: PROCEEDINGS

www.materialstoday.com/proceedings

DAS35

Numerical and experimental investigation of contact length during orthogonal cutting

Szabolcs Berezvai*, Tamas G. Molnar, Attila Kossa, Daniel Bachrathy, Gabor Stepan

Budapest University of Technology and Economics, Faculty of Mechanical Engineering, Department of Applied Mechanics, Műegyetem rkp. 5., Budapest H-1111, Hungary

Abstract

In this paper, the influence of the chip thicknesses on the contact length between the rake face of the tool and the chip is investigated during orthogonal cutting. This is an important parameter in metal cutting, since it determines the cutting force over the rake face and the heat transfer between the tool and the workpiece. Therefore, it plays significant role in the theoretical cutting force models and in the dynamics of cutting processes. This paper is dedicated to determine the contact length based on experimental methods and finite element analysis (FEA) using the so-called Coupled Eulerian-Lagrangian (CEL) formulation.

Selection and peer-review under responsibility of 35th Danubia Adria Symposium on Advances in Experimental Mechanics.

Keywords: Metal cutting; Chip formation; Contact length; CEL simulation;

1. Introduction

The achievable productivity of the metal cutting processes may be limited by the occurrence of undesired and harmful self-excited vibrations, called as machine tool chatter. Furthermore, chatter may also lead to poor surface quality and increased tool wear. Therefore, there is significant need to understand the dynamics of cutting and eliminate chatter. In the mechanical models of metal cutting, this phenomenon is usually explained by the so-called surface regenerative effect [1-4]. These models rely also on theoretical cutting force expressions, which describe the interaction between the tool and the workpiece. Consequently, modelling and measuring this interaction is important in terms of developing accurate cutting force models and to investigate the dynamics of cutting [5].

* Corresponding author. Szabolcs Berezvai. Tel.: +36-1-463-1235; fax: +36-1-463-1369.
E-mail address: berezvai@mm.bme.hu

Selection and peer-review under responsibility of 35th Danubia Adria Symposium on Advances in Experimental Mechanics.

The interaction between the hot chip and the tool surface can be characterized by the contact length, which is the distance over which the tool remains in contact with the freshly formed chip. This is an important parameter, since it determines the heat transfer between the tool and the chip, which dominates tool wear. Additionally, since the cutting force is the resultant of a force system distributed along the rake face of the tool, the contact length also plays an important role in the cutting force models and affects the occurrence of machine tool chatter [5]. The simplest machining operation, where the chip formation process and the variation of the contact length can be investigated, is orthogonal cutting realized by planing process [6,7].

The goal of this contribution is to compare theoretical contact length models to experiments using image processing method and finite element (FE) simulations. In the literature, FE simulations of the chip formation process using the so-called Coupled Eulerian-Lagrangian (CEL) technique is becoming increasingly popular. In this formulation the tool is described by the Lagrangian formulation, while the workpiece by the Eulerian one. This ensures that no mesh distortion problems occur and the element deletion can also be avoided [8,9].

The outline of the paper is the following: in Section 2, the most common applied contact length models are reviewed. The details of the planing tests and the image processing method are provided in Section 3, while Section 4 discusses the FE simulations using the CEL approach. The comparison of the theoretical model predictions and the FE simulations are presented in Section 5, while the results of the paper are concluded in Section 6.

2. Theoretical contact length models

According to the mechanical model of orthogonal cutting, as presented in Figure 1, the chip formation process can be described using three distinguished deformation zones. Initially, the uncut workpiece material in front of the tool is sheared over the primary zone and forms chip. Assuming rigid – perfectly plastic material behavior for the workpiece and perfectly sharp tool tip, the shear zone can be modelled as a plane located at shear angle ϕ_c measured from the direction of the cutting speed v_c. Then, in the secondary zone the chip undergoes further deformation as it moves over the rake face of the tool, which can be characterized by the contact length L_c. The tertiary zone is the friction area of the flank face of the tool and the freshly machined surface.

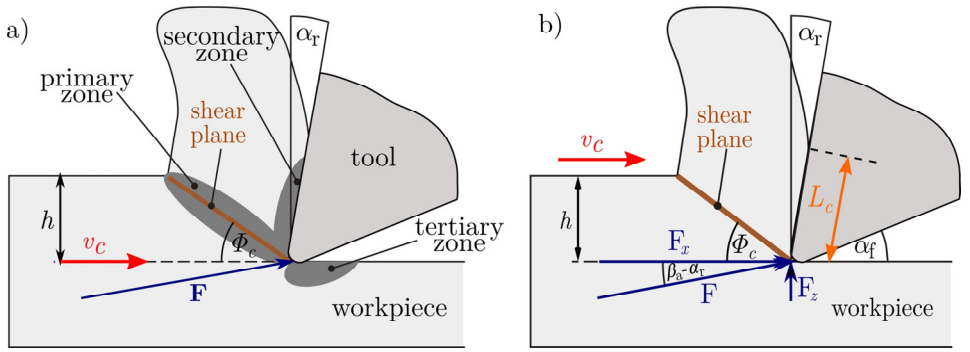

Fig. 1. The model of orthogonal cutting with (a) the deformation zones and (b) the contact forces and contact length

The geometry of the tool can be characterized by the rake angle α_r and the flank angle α_f while h denotes the uncut chip thickness. The horizontal and vertical components of the cutting force **F** can be obtained using the average friction angle β_a, for which $\beta_a - \alpha_r = \arctan(F_z / F_x)$ holds [1].

In the literature several contact length models are available, most of them were developed experimentally and determine the contact length as a function of the undeformed chip thickness h. The most commonly applied models (Altintas [1], Lee and Schaffer, Vinogradov [5]), are very similar in their mathematical form and dependent on the shear angle ϕ_c and the tool geometry as

$$L_c^{\text{Alt}} = \frac{h\sin(\phi_c + \beta_a - \alpha_r)}{\sin\phi_c \cos\beta_a}, \tag{1}$$

$$L_c^{\text{Vinogr}} = \frac{h\sin(\pi/4)}{\sin\phi_c \sin(\pi/4 + \phi_c - \alpha_r)}, \tag{2}$$

$$L_c^{\text{Lee}} = \frac{2h\sin(\pi/4)}{\sin\phi_c \sin(\pi/4 + \phi_c - \alpha_r)}, \tag{3}$$

where the shear angle ϕ_c can be modelled based on the minimum energy principle (MEP) or the maximum shear stress principle (MSSP) as [1]

$$\phi_c^{\text{MSSP}} = \frac{\pi}{4} - (\beta_a - \alpha_r), \text{ and } \phi_c^{\text{MEP}} = \frac{\pi}{4} - \frac{\beta_a - \alpha_r}{2}. \tag{4}$$

Note, that in case of applying shear angle model based on MSSP, the estimation of Altintas and Vinogradov in Eqs. (1)-(2) are identical, while the model of Lee in Eq. (3) differs only in a multiplier of 2. However, assuming MEP shear angle model, the estimation of expressions are different.

3. Experimental layout and methods

Orthogonal planing tests were conducted in order to determine experimentally the relationship between the uncut chip thickness h and the chip-tool contact length L_c [6,7]. The tests (see Figure 2/a) were performed on a single aluminum (A2024-T351) rib of thickness $w = 2$ mm using the feed motion of a NCT EmR-610Ms CNC milling machine with cutting speed $v_c = 10,000$ mm/min. The cutting force components in the (x-y-z) coordinate system were measured using KISTLER 9129 AA dynamometer. During the cutting tests carbide tools were applied with rake angle $\alpha_r = 15^\circ$ and $\alpha_f = 10^\circ$, while the uncut chip thickness h was set between $h_{\min} = 0.05$ mm and $h_{\max} = 0.25$ mm using steps of $\Delta h = 0.01$ mm.

Additionally, the tool was covered with black painting, which the chip removed during cutting (see Figure 2/b). This allowed the estimation of the maximal contact length denoted as L_c^{IA} via image analysis (see Figure 2/c), which was performed on high-resolution photos taken with Canon EOS Mark III 5D camera and Canon MP-E 65 mm macro lens. In the first step of the algorithm the right corner of the tool was detected and from that point a small slice including the rake face of the tool was cropped and binarized to black and white. Finally, the profile of the black area was obtained by summing the black pixels in each columns, which indicated the maximal contact length.

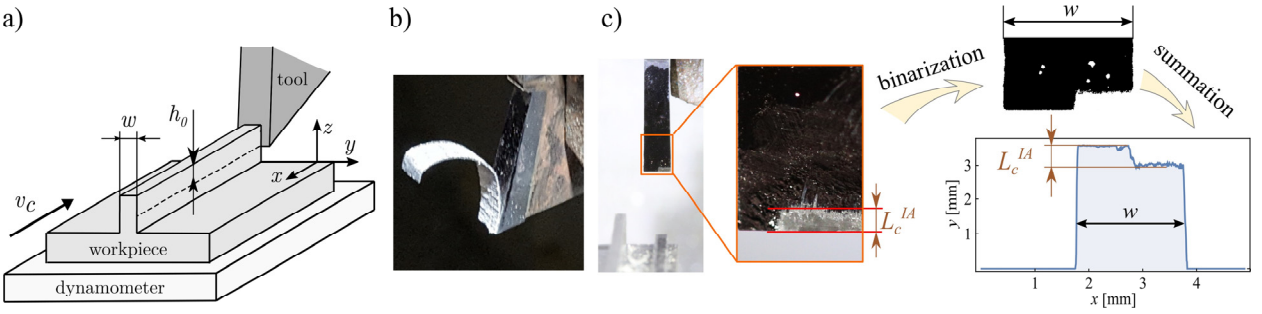

Fig. 2. (a) The measurement layout of the orthogonal cutting test; (b) the freshly formed chip in contact with the tool and the removed painting of the rake face of the tool; (c) the image processing algorithm applied to determine the maximal contact length values for each depth of cut

4. Finite element simulations

In order to validate the contact length models, finite element (FE) simulations of the planing process were performed. In the FE model (see Fig. 3.) Coupled Eulerian-Lagrangian (CEL) approach was applied for the tool-workpiece system using explicit, dynamic simulation with coupled temperature-displacement formulation. The CEL approach was originally developed to study fluid-structure interactions, however recently it has already been applied to simulate metal cutting and investigate the chip formation process [8,9].

Since in the commercial finite element software Abaqus (version 2018) [10] only 3D elements are available for explicit simulations using CEL, only two elements were used out of the cutting plane (in *y*-direction) to reduce the computational time, while plane strain conditions were ensured by applying symmetry boundary conditions on all *x-z* planes.

At the beginning of the simulation a portion of the initial Eulerian void was filled with the workpiece material (see the dark-gray shaded area in Figure 3/a), for which constant speed of 10,000 mm/min was prescribed. During the simulation the Eulerian void fraction (EVF) was tracked in each cell, which indicates the ratio of the material inside the element to the total volume of that Eulerian cell. Therefore, EVF=0 means a totally empty cell, while EVF=1 is an element which completely filled with the workpiece material.

The geometry of the Lagrangian tool was built in accordance with the tool geometry applied in the cutting tests, where the cutting edge radius was 35 µm. In order to investigate the contact pressure distribution, the tool was placed in the Eulerian void in a way, that for the highest depth of cut values the curved chip and the total contact are still remained in the initial Eulerian void. The mesh was composed of 3D 8-node brick elements: linear Eulerian bricks with reduced integration (EC3D8R) and thermally coupled bricks with trilinear displacement and temperature and reduced integration (C3D8RT). The CEL model totaled 12720 nodes (tool: 1206, workpiece 11514) and 6326 elements (tool: 726, workpiece: 5600), which is illustrated in Figure 3/b.

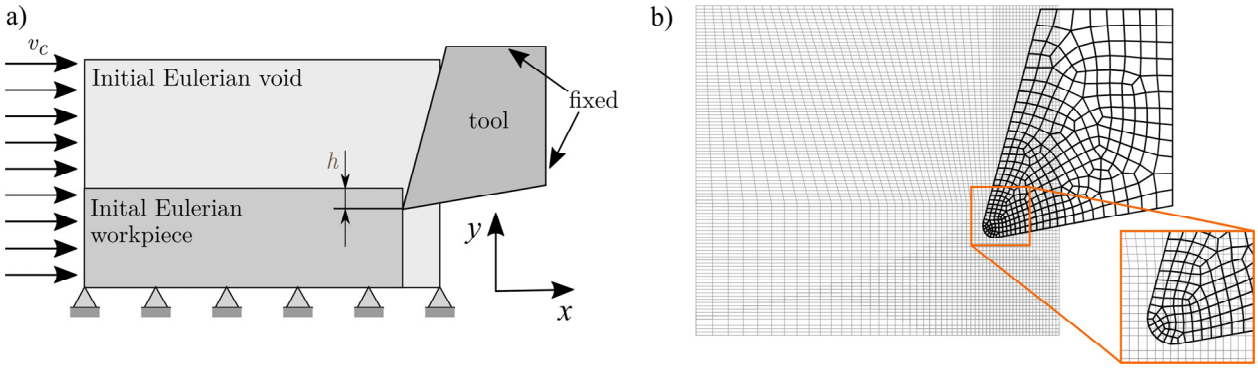

Fig. 3. (a) The FE model using CEL formulation; (b) the initial mesh of the model

The mechanical behavior of the carbide tool was modelled as elastic, while workpiece material was characterized by the Johnson-Cook viscoplastic model in combination with the Johnson-Cook damage model using fracture energy based damage evolution. The model defines the yield stress at nonzero strain rate as

$$\bar{\sigma} = \left[A + B(\bar{\varepsilon}^{pl})^n\right]\left[1 + C\ln\left(\frac{\dot{\bar{\varepsilon}}^{pl}}{\dot{\varepsilon}_0}\right)\right]\left[1 - \left(\frac{T - T_0}{T_m - T_0}\right)^m\right], \tag{6}$$

where $\bar{\varepsilon}^{pl}$ is the equivalent plastic strain, T_m is the melting temperature, T_0 is room-temperature, $\dot{\varepsilon}_0$ is the reference strain rate, while *A, B, C, m* and *n* are material parameters [8-10].

According to the Johnson-Cook damage model the equivalent plastic strain at the onset of the damage is expressed as

$$\bar{\varepsilon}_D^{pl} = \left[d_1 + d_2 \exp(-d_3\eta)\right]\left[1 + d_4 \ln\left(\frac{\dot{\bar{\varepsilon}}^{pl}}{\dot{\varepsilon}_0}\right)\right], \tag{7}$$

where η is the stress triaxility, while d_1, d_2, d_3 and d_4 are the corresponding material parameters [10]. The material parameters applied in the CEL simulations are summarized in Tables 1-3.

Table 1. Elastic and thermal parameters of the carbide tool and the aluminum workpiece

	Young's modulus E [GPa]	Poisson's ratio ν [-]	Density ρ [kg/m^3]	Conductivity k [W/mK]	Expansion α [1/K]	Specific heat c_p [J/kgK]
Carbide	800	0.3	15000	46	4.7e-6	203
A2024-T351	73	0.33	2700	121	2.28e-5	875

Table 2. Viscoplastic Johnson-Cook parameters of A2024-T351

	A [MPa]	B[MPa]	C	m	n	$\dot{\varepsilon}_0$	T_0 [K]	T_m [K]
A2024-T351	352	440	0.0083	1	0.42	0.000333	298	793

Table 3. Johnson-Cook damage parameters of A2024-T351

	d_1	d_2	d_3	d_4	$\dot{\varepsilon}_0$	Fracture Energy [mJ]
A2024-T351	0.13	0.13	1.5	0.11	1	12

For the friction between the tool and the workpiece Coulomb friction was adopted with friction coefficient of $\mu = 0.2$ assuming that 100% percent of the dissipated frictional energy is converted to heat, which is distributed equally between the parts (heat partition was 50-50%). The total simulation time was $t = 0.01$ s.

5. Results

In case of each cutting test, the measured force signals were averaged and the mean values of the components F_x and F_z were obtained. Then, the corresponding average friction angles were calculated for each depth of cut values using the relation $\beta_a = \arctan(F_z / F_x) + \alpha_r$. The variation of the friction angle as the function of h shows slight decrease as the depth of cut increases (see Figure 4/a).

As a next step, the contact length and shear angle values could be expressed using the models in Eqs. (1)-(3) and Eqn. (4), respectively (see markers in Figure 4/c.). Due to the slight variation in the fraction angle, all the contact length expressions as a function of the uncut chip thickness show linear characteristics. Additionally, it can be seen that the models based on the MSSP shear angle model always overestimate the predictions relying on the MEP. It should be noted, that the estimation of the shear angle using the MEP always results in larger and more accurate shear angle, as it was concluded previously based on high-speed camera recordings [6,7].

Moreover, the contact length was also obtained from the FE simulations using the contact pressure distribution along the rake face of the tool (see Figure 4/d.) where the contact length was indicated by the area of nonzero contact pressure. The results were compared to the predictions of the theoretical expressions and the image analysis, which is presented in Figure 4. The comparison of the theoretical predictions and results of the CEL simulations revealed, that the Lee and Shaffer model using MEP shear angle model shows perfect correspondence at small values of the chip thickness h. In case of high h values, the discrepancy between the models becomes more significant. This can be explained through the phenomenon of chip segmentation which starts to occur above chip thicknesses $h > 0.1$ mm (denoted by blue shading in Figure 4/a-c), which can be also indicated by the increased standard deviation of the contact length in Figure 4/b.

Furthermore, the results of the CEL simulations can be validated using the maximal contact length values obtained from the experiments by image analysis (see Figure 4/a). The results show great correspondence with CEL simulations especially at small chip thicknesses.

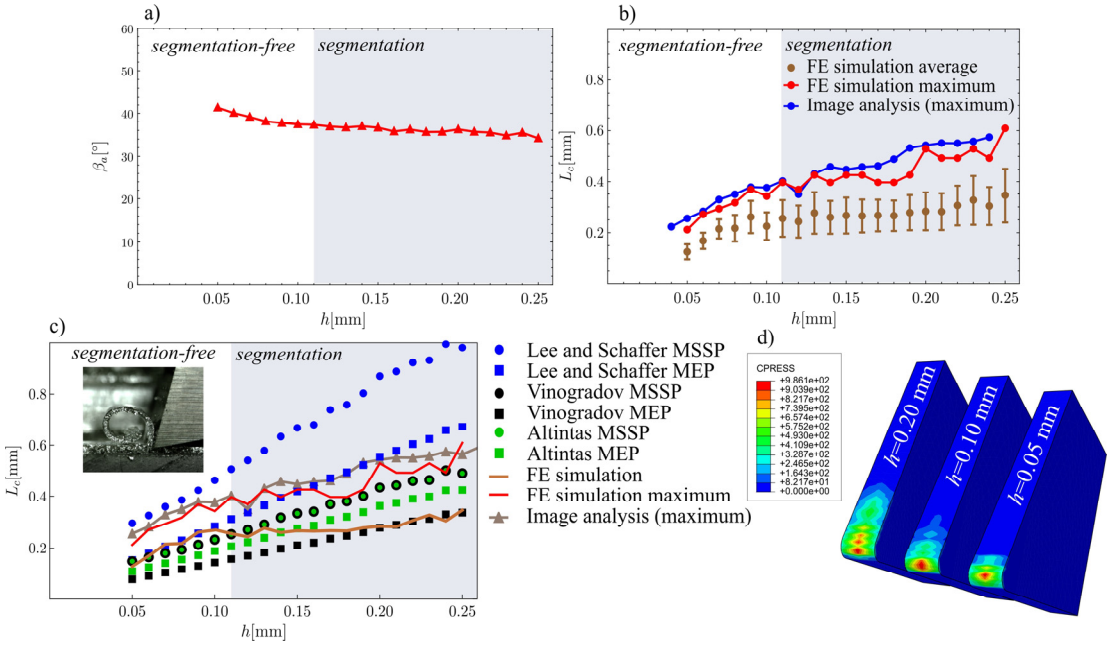

Fig. 4. (a) Variation of the average friction angle; (b) The mean and maximal contact length values obtained by CEL in comparison with the image processing; (c) Comparison of the contact length estimations; (d) Contact pressure distribution in case different depth of cut values;

6. Conclusion

It can be concluded, that the contact length can be estimated by theoretical expressions based on orthogonal cutting test and by FE simulations using the Coupled Eulerian-Lagrangian formulation. The experiments also revealed that the average contact length values obtained by FE simulations are in good agreement with the prediction of the Lee and Shaffer model based on the MEP shear angle model. At higher values, however, the discrepancy between the models and the experiments becomes more significant due to the occurrence of chip segmentation. Therefore, in that region the theoretical models become less accurate and reliable.

Acknowledgements

This research has been supported by the ÚNKP-18-3-I. New National Excellence Program of the Ministry of Human Capacities, Hungary. The research leading to these results has received funding from the European Research Council under the European Union's Seventh Framework Programme (FP/2007-2013) / ERC Advanced Grant Agreement n. 340889.

References

[1] Y. Altintas, Manufacturing Automation - Metal Cutting Mechanics, Machine Tool Vibrations and CNC Design, second ed., Cambridge University Press, Cambridge, 2012.
[2] G. Stepan, Retarded Dynamical Systems: Stability and Characteristic Functions, Longman, Harlow, 1989
[3] E. Budak, Y. Altintas, J Dyn Syst Meas Contr. 120 (1998) 22-30.
[4] G. Stepan, in: F. C. Moon (Ed.), Dynamics and Chaos in Manufacturing Processes, John Wiley and Sons, New York, 1998, pp. 165-192.
[5] S.A. Iqbal, P.T. Mativenga, M.A. Sheikh, Int J Adv Manuf Tech. 42 (2009) 30–40.
[6] S. Berezvai, D. Bachrathy, G. Stepan, Mater Today-Proc. 5 (2018) 26495-26500.
[7] S. Berezvai, TG. Molnar, D. Bachrathy, G. Stepan, Proc CIRP. 77 (2018) 155-158
[8] F. Ducobu, E. Riviere-Lorphevre, E. Filippi, Eur J Mech A Solids. 59 (2016) 58-66.
[9] F. Ducobu, E. Riviere-Lorphevre, E. Filippi, Finite Elem Anal Des. 134 (2017) 27-40.
[10] Dassault Systemes, Abaqus, version 2018.